



# MgO-Coated Layered Cathode Oxide With Enhanced Stability for Sodium-Ion Batteries

Ling Xue<sup>2</sup>, Shuo Bao<sup>2</sup>, Ling Yan<sup>3</sup>, Yi Zhang<sup>1</sup>, Jinlin Lu<sup>1\*</sup> and Yansheng Yin<sup>1\*</sup>

<sup>1</sup>Research Center for Corrosion and Erosion Process Control of Equipment and Material in Marine Harsh Environment, Guangzhou Maritime University, Guangzhou Guangdong, China, <sup>2</sup>School of Materials and Metallurgy, University of Science and Technology, Liaoning, Anshan, China, <sup>3</sup>State Key Laboratory of Metal Material for Marine Equipment and Application, Anshan, China

$\text{Na}_{0.67}\text{Ni}_{0.33}\text{Mn}_{0.67}\text{O}_2$  is a prospective layered cathode material for sodium-ion batteries owing to its low cost, ease of synthesis, and high specific capacity. However, due to direct contact with electrolytes during the cycling process, the cyclic stability is not satisfied. To address this issue, magnesium oxide (MgO) surface modification was performed in this study to improve the material's cycling properties. MgO layers of various thicknesses were successfully coated onto the cathode, and their electrochemical performances were thoroughly investigated. Among the as-prepared samples, the 2 wt% MgO-coated sample demonstrated the best rate capability and cycling stability. It had an initial reversible discharge capacity of  $105 \text{ mAh g}^{-1}$  in the voltage range from 2.0 to 4.5 V at 0.2 C with a high cycle retention of 81.5%. Electrochemical impedance spectroscopy (EIS) results showed that the 2 wt% MgO-coated electrode had the highest conductivity due to the smaller charge transfer resistance (Rct) value. All the test results show that the MgO modification improves the electrochemical properties of  $\text{Na}_{0.67}\text{Ni}_{0.33}\text{Mn}_{0.67}\text{O}_2$  cathode material. This research could lead to the development of a promising strategy for improving the electrochemical performance of next-generation sodium-ion batteries.

## OPEN ACCESS

### Edited by:

Renheng Wang,  
Shenzhen University, China

### Reviewed by:

Feng Gu,  
Jiangxi University of Science and  
Technology, China  
Lidong Sun,  
Chongqing University, China

### \*Correspondence:

Jinlin Lu  
jinlinlu@hotmail.com  
Yansheng Yin  
ysyin@shmtu.edu.cn

### Specialty section:

This article was submitted to  
Electrochemical Energy Conversion  
and Storage,  
a section of the journal  
Frontiers in Energy Research

Received: 03 January 2022

Accepted: 24 January 2022

Published: 28 February 2022

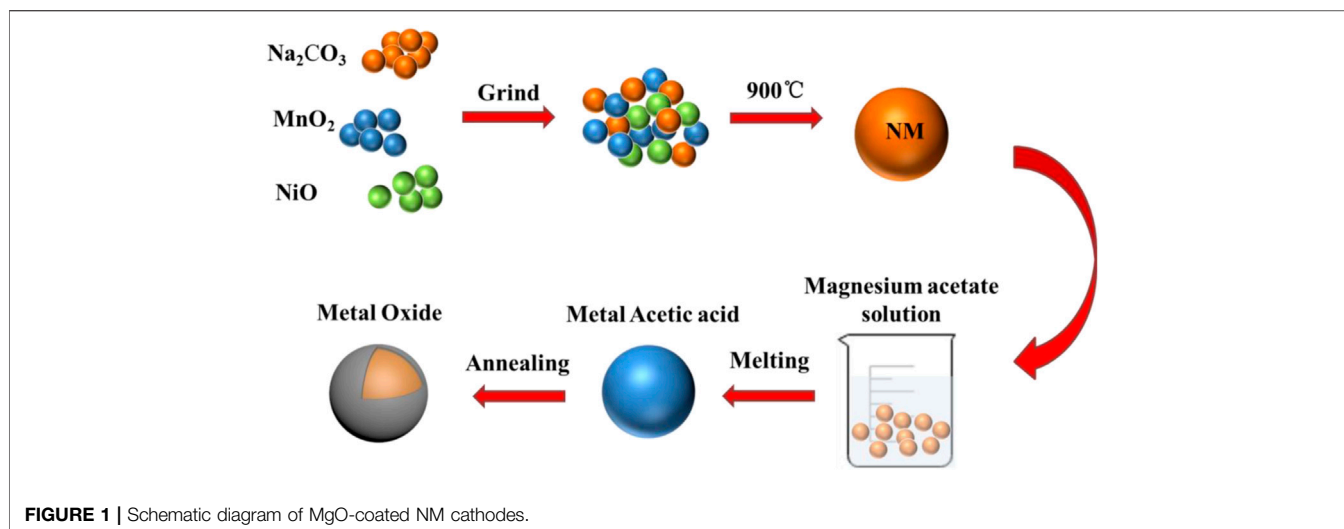
### Citation:

Xue L, Bao S, Yan L, Zhang Y, Lu J and  
Yin Y (2022) MgO-Coated Layered  
Cathode Oxide With Enhanced  
Stability for Sodium-Ion Batteries.  
Front. Energy Res. 10:847818.  
doi: 10.3389/fenrg.2022.847818

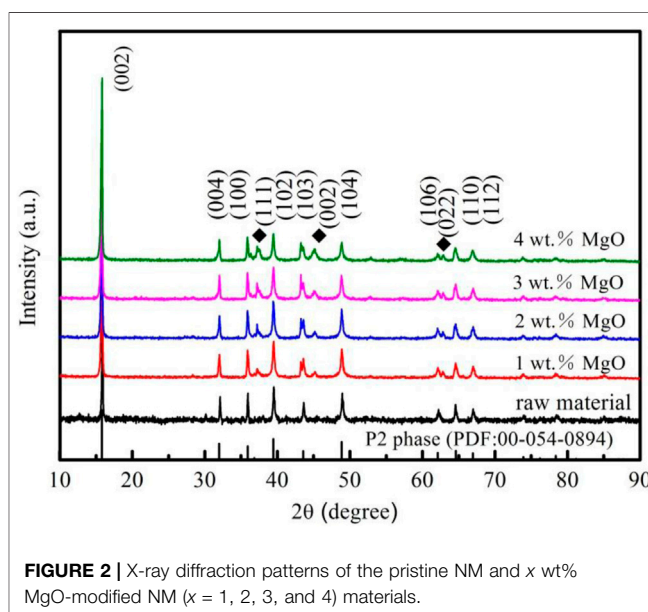
**Keywords:** sodium-ion battery, layered cathode oxide materials, MgO modification,  $\text{Na}_{0.67}\text{Ni}_{0.33}\text{Mn}_{0.67}\text{O}_2$ , electrochemical properties

## INTRODUCTION

Recently, the rapid development of electronic equipment and low-power electric vehicles has increased the demand for energy storage materials with high energy efficiency, abundant resources, and environmental friendliness (Kundu et al., 2015; González et al., 2016). Lithium-ion batteries (LIBs) are currently recognized as an energy storage product with high energy density and good performance rating. However, given the massive consumption of lithium batteries, the shortage of lithium resources will inevitably be a serious problem (Lu et al., 2013; Peng et al., 2016). In contrast, sodium-ion batteries (SIBs) have the advantages of a wider source of raw materials, lower cost, and more safety than LIBs. In some energy storage fields with low energy density requirements, the shortage of lithium resources can be alleviated to a certain extent (Pu et al., 2019; Hakim et al., 2021). Moreover, the electrochemical performance of SIBs is mainly determined by the cathode material. Prussian blue analogues (Zhu et al., 2019; Du and Pang, 2021), organic compounds (Wang et al., 2014; Huang et al., 2017), polyanionic compounds (Essehli et al., 2020; Lv et al., 2021), and layered transition metal oxide (Yang and Wei, 2020; Zhao et al., 2021) as SIB cathode materials have been extensively researched. Most of them have the fatal issue of low average working voltage, which



severely restricts their energy density. Among them, layered transition metal oxides ( $\text{Na}_x\text{MO}_2$ ) with high operating voltage and electrochemical capacity, such as P2-type (Kuan Wang et al., 2018; Kannan et al., 2021) and O3-type cathode materials (Rong et al., 2019), are deemed promising cathode material candidates for commercialization. Among many layered oxides, P2- $\text{Na}_{2/3}[\text{Ni}_{1/3}\text{Mn}_{2/3}]\text{O}_2$  has been the focus of research because of its low cost, ease of synthesis, and high theoretical capacity of more than  $250 \text{ mAh g}^{-1}$  (Wu et al., 2015). However, an experimental study shows that the irreversible phase transition and volume change of P2 to O2 phase can be observed when charging to 4.2 V, resulting in poor cycling stability, thereby leading to a great restriction for its practical application (Lee et al., 2013; Peng-Fei Wang et al., 2018). Under high voltage, the electrolyte is easily decomposed into hydrofluoric acid and water molecular impurities, resulting in the corrosion of active substances, which makes the cathode material unable to transport ions, and the disembedding of  $\text{Na}^+$  at high voltage also destroys the crystal structure, eventually decreasing cycling stability (Tanabe et al., 2013). To enhance the cycling stability of P2-type cathode materials, many efforts have been made, such as doping transition metals (Jin et al., 2020; Zhao et al., 2020; Devendrasinh et al., 2021). For example, Wang et al. (2016) prepared Mn and Ni matrix P2- $\text{Na}_{0.67}\text{Mn}_{0.67}\text{Ni}_{0.23}\text{Mg}_{0.05}$  using the sol-gel method, which maintained good structural stability and retained about 85% reversible capacity after 50 cycles. Besides doping, surface modification is another effective method of improving electrochemical performance. Various metal oxides and phosphate coatings [ $\text{Al}_2\text{O}_3$  (Kaliyappan et al., 2015),  $\text{CuO}$  (Dang et al., 2019),  $\text{ZrO}_2$  (Kaliyappan et al., 2017),  $\text{ZnO}$  (Yang et al., 2020),  $\text{TiO}_2$  (Yu et al., 2020),  $\text{NaPO}_3$  (Jae Hyeon Jo et al., 2018), and  $\text{NaCaPO}_4$  (Chang-Heum Jo et al., 2018)] have been applied to various anodes and cathodes to achieve the application of high-performance SIBs. Kaliyappan et al. (2015) coated  $\text{Al}_2\text{O}_3$  with different thicknesses on the surface of P2- $\text{Na}_{2/3}(\text{Mn}_{0.54}\text{Ni}_{0.13}\text{Co}_{0.13})\text{O}_2$  using atomic layer deposition technology. The samples showed good electrochemical properties. The maximum discharge



capacity of MNC-2 electrode material at 1 C is  $123 \text{ mAh g}^{-1}$ , and the cycling stability of the material is better than that of pristine material.  $\text{Al}_2\text{O}_3$  coating has been proven to be able to effectively improve the cycling stability of the cathode materials. Dang et al. (2019) coated a layer of  $\text{CuO}$  on the surface of P2- $\text{Na}_{2/3}\text{Ni}_{1/3}\text{Mn}_{2/3}\text{O}_2$ , which not only improved the structural stability but also reduced the decomposition degree of the material at high potential. Electrochemical tests showed that the specific capacities of  $\text{Na}_{2/3}\text{Ni}_{1/3}\text{Mn}_{2/3}\text{O}_2$  at 0.1 and 5 C were 101 and  $45 \text{ mAh g}^{-1}$ , respectively. The specific capacities of coated  $\text{Na}_{2/3}\text{Ni}_{1/3}\text{Mn}_{2/3}\text{O}_2$  at the same rate were 107 and  $69 \text{ mAh g}^{-1}$ , and the coated samples showed higher capacity and cycling stability. Therefore, as regards layered cathode oxide SIBs, an effective coating can reduce the contact with electrolyte, alleviate electrode dissolution, and enhance the cycling stability.

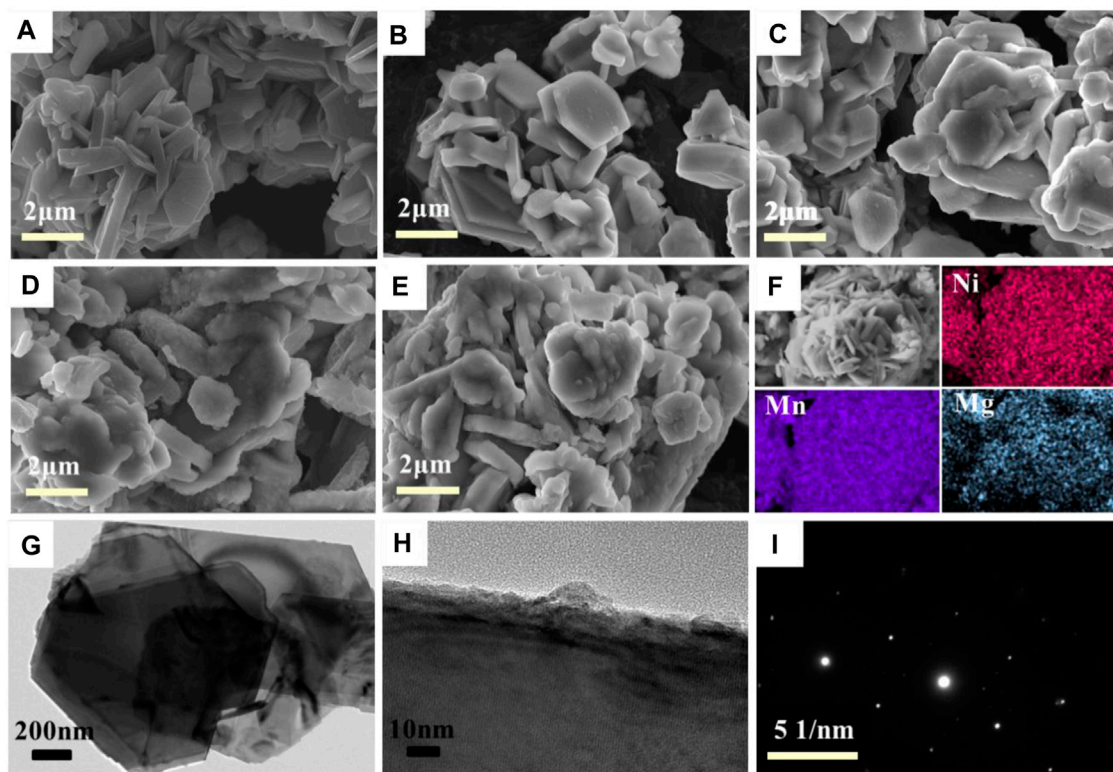


**FIGURE 3** | SEM images of MgO-coated samples [(A) 0 wt%; (B) 1 wt%; (C) 2 wt%; (D) 3 wt%; (E) 4 wt%]. (F) EDX mappings of Ni, Mn, and Mg in 2 wt% MgO-coated samples, (G) TEM image, (H) HRTEM image, and (I) SAED patterns of a single particle of 2 wt% MgO-coated samples.

In this study, the  $\text{Na}_{0.67}\text{Ni}_{0.33}\text{Mn}_{0.67}\text{O}_2$  sample was prepared by a simple solid-state method, and a facile wet chemistry route method was used to fabricate a MgO-coated  $\text{Na}_{2/3}\text{Ni}_{1/3}\text{Mn}_{2/3}\text{O}_2$  composites. MgO layers of various thicknesses were successfully coated onto the layered cathode oxide  $\text{Na}_{0.67}\text{Ni}_{0.33}\text{Mn}_{0.67}\text{O}_2$ , and the quantity of MgO was optimized. MgO coating significantly improves the cyclic stability and rate capability of pristine  $\text{Na}_{0.67}\text{Ni}_{0.33}\text{Mn}_{0.67}\text{O}_2$  because it effectively alleviates electrode dissolution and stabilizes the structure of the electrode. This research demonstrates that MgO modification is an effective strategy for improving the electrochemical performance of layered cathode oxide and expands the potential commercial applications of layered cathode oxide.

## MATERIALS AND METHODS

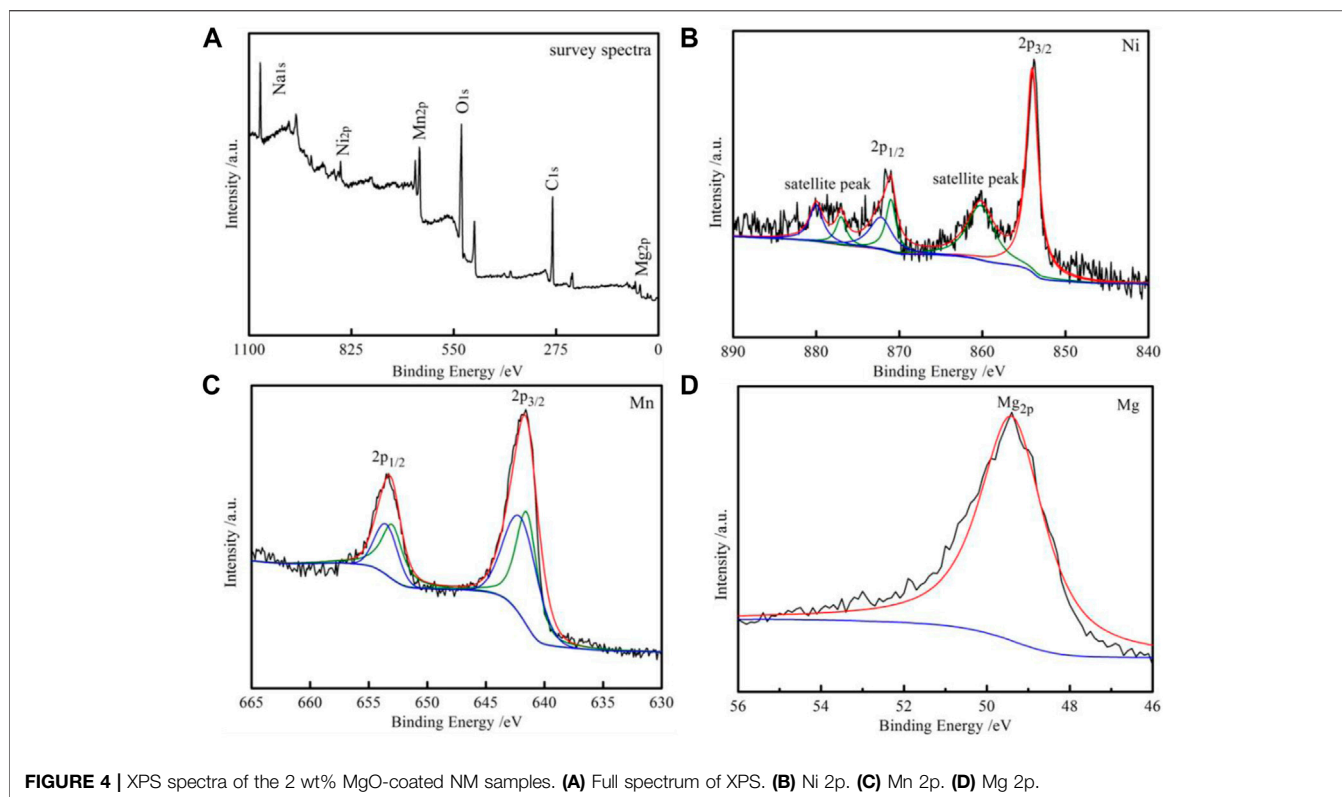
### Synthesis

Firstly,  $\text{Na}_{0.67}\text{Ni}_{0.33}\text{Mn}_{0.67}\text{O}_2$  (NM) was prepared by a facile solid-state reaction. Sodium carbonate, magnesium oxide, nickel oxide, and manganese oxide were mixed according to the stoichiometric ratio. The mixture with 0.3865 g  $\text{Na}_2\text{CO}_3$ , 0.5825 g  $\text{MnO}_2$ , and 0.2134 g NiO was calcined at  $900^\circ\text{C}$  for 12 h to acquire the pristine NM sample. The MgO with different thicknesses was coated on NM using a facile wet chemistry route. For example, 0.053 g of magnesium was firstly acetated in a beaker containing 50 ml

alcohol. Then, 1 g of NM was added with stirring for 2 h. The mixed solution was dried in an oven at  $80^\circ\text{C}$  for 5 h. The dried powder was heated in air at  $550^\circ\text{C}$  for 5 h to obtain 1 wt% MgO-coated NM sample. The 2, 3, and 4 wt% MgO-coated NM samples were synthesized through the same procedure only using the different weights of magnesium.

### Characterization

XRD patterns were collected on X-ray diffraction (Rigaku) with Cu  $K\alpha$  radiation ( $\lambda = 0.154060$  nm) within the  $2\theta$  between  $10^\circ$  and  $90^\circ$  at  $4^\circ$  per minute. The evaluation of particle morphology and element distribution was performed using scanning electron microscopy (SEM; ZEISS SUPRA55). TEM (JEM2100) images were used to perform the evaluation of morphology and microstructure of cathode materials. XPS (Axis Ultra DLD) was applied to observe the valence states of Ni, Mn, and Mg elements. The active cathode materials were mixed uniformly with carbon black and polyvinylidene fluoride (PVDF) in N-methyl pyrrolidone (NMP) at a mass ratio of 8:1:1. After mixing and stirring for 2 h, the slurry was uniformly smeared onto Al foils and dried in a vacuum oven at  $120^\circ\text{C}$  for 10 h. The mass loading of the active materials was about  $2\text{ mg cm}^{-2}$ . The electrolyte was 1 M  $\text{NaClO}_4$  dissolved in propylene carbonate/fluoroethylene carbonate (19:1 in volume). Then, the as-prepared cathode, sodium discs (Aldrich, >99%), and glass fiber (Whatman) were assembled into the CR2032-type coin cell in



glove box. Current–voltage (CV) curves were performed on a CHI1000C electrochemical workstation (Chenhua) at a scan rate of  $0.1 \text{ mV s}^{-1}$ , and electrochemical impedance spectroscopy (EIS) was measured with a voltage amplitude of 5 mV for the scanning turns for three cycles. Charge/discharge, rate, and long-term cycling properties were analyzed by Land Instruments (Wuhan, China) in a voltage range of 2–4.5 V at room temperature.

## RESULTS AND DISCUSSION

MgO-coated NM composites are obtained by a facile wet chemistry route method. The synthesis procedure is described in **Figure 1**. The NM is prepared by high-temperature solid-state process. The MgO coating is obtained from magnesium acetate solution to stabilize the structure of the material.

The XRD spectra of the samples are presented in **Figure 2**. The reflection peaks located at  $15.7^\circ$ ,  $35.9^\circ$ , and  $43.5^\circ$  are consistent with the (002), (100), and (103) planes for different thicknesses of MgO/NM cathode materials, which conforms to the P2 structure (JCPDS No. 00-05-0894) of electrodes. Furthermore, the peaks located at  $2\theta = 37.13^\circ$ ,  $43.1^\circ$ , and  $62.6^\circ$  correspond to (111), (002), and (022) crystal planes of MgO (JCPDS No. 96-901-3247). The above results indicate that the MgO and P2 structures of NM cathode materials are successfully prepared.

The morphologies of samples are investigated by SEM and TEM. **Figure 3A–E** displays that all samples exhibit hexagonal

sheets and a particle size of  $\sim 1\text{--}4 \mu\text{m}$ . X-ray spectrometry elemental mapping is used to indicate that elements exist on the surface of NM cathode along with MgO in **Figure 3F**. TEM images (**Figure 3G, H**) of 2 wt% MgO-coated samples show that the morphologies of secondary particles in SEM and TEM are comparable. The MgO surface coating is evidently observed in the high-resolution TEM images, and it can be observed that MgO is greatly coated on the surface with an obvious boundary between the bulk and surface. Selected area electron diffraction (SAED) images of 2 wt% MgO-coated samples are shown in **Figure 3I** with continuous diffraction rings, indicating the P2-type structure of samples. All results confirm that an MgO-coated layer is successfully synthesized.

XPS spectra of 2 wt% MgO-coated samples are presented in **Figure 4** to analyze the valence states of elements. It can be found that there are Na, Mn, Ni, Mg, C, and O elements in the entire spectrum of XPS in **Figure 4A**. In **Figure 4B**, two binding energy peaks near 854 and 871 eV represent Ni  $2p_{3/2}$  and Ni  $2p_{1/2}$ , implying the +2 valence state of Ni ion (Lin et al., 2015), and the weaker satellite peaks at  $\sim 881$  and  $\sim 861$  eV indicate the presence of  $\text{Ni}^{3+}$  (Bao et al., 2021). Two domain peaks are divided into four peaks in **Figure 4C**; the couple of peaks at 641 and 653 eV represents  $\text{Mn}^{3+}$ , whereas the couple of peaks located at 642 and 653.5 eV can be ascribed to  $\text{Mn}^{4+}$  (Li et al., 2013). The spectra of Mg 2p observed at the binding energy of 49 eV of the 2 wt% MgO-coated materials are shown in **Figure 4D**. The binding energy of Mg corresponds to MgO, implying a +2 oxidation state for Mg (Shi et al., 2013).

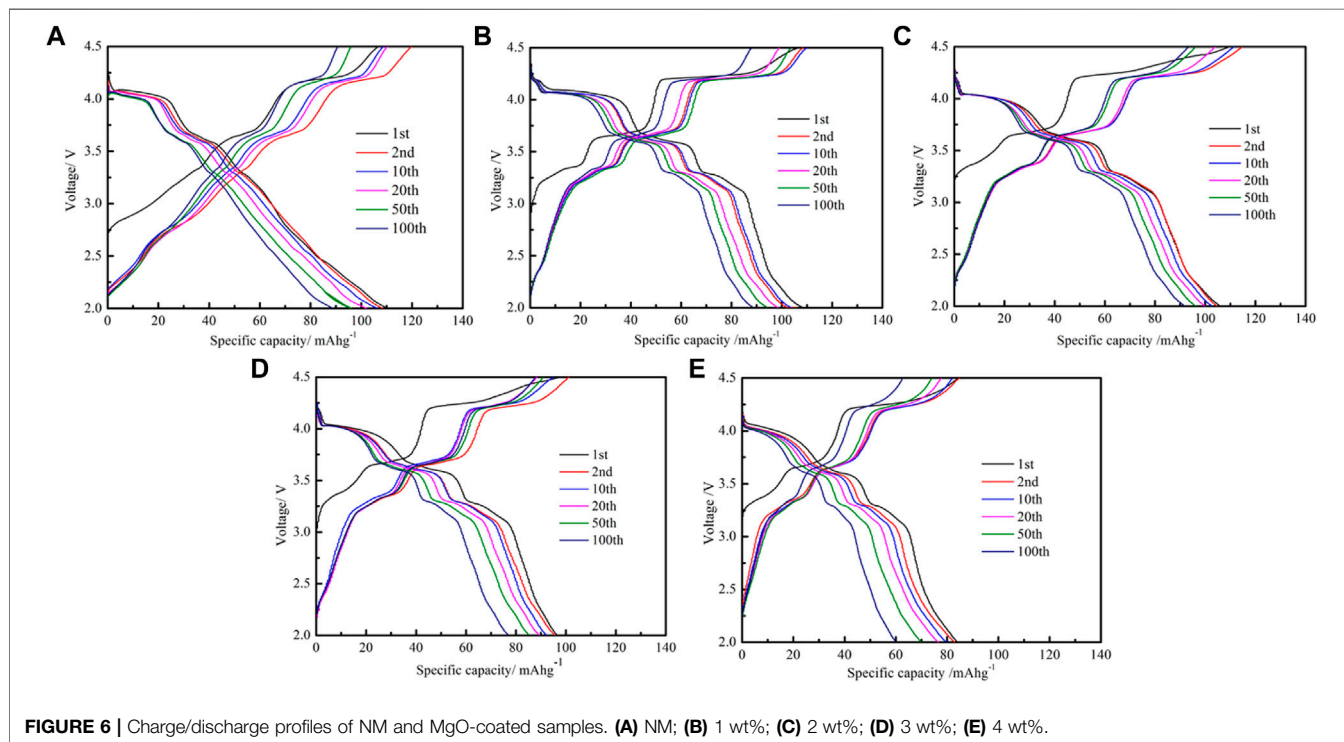
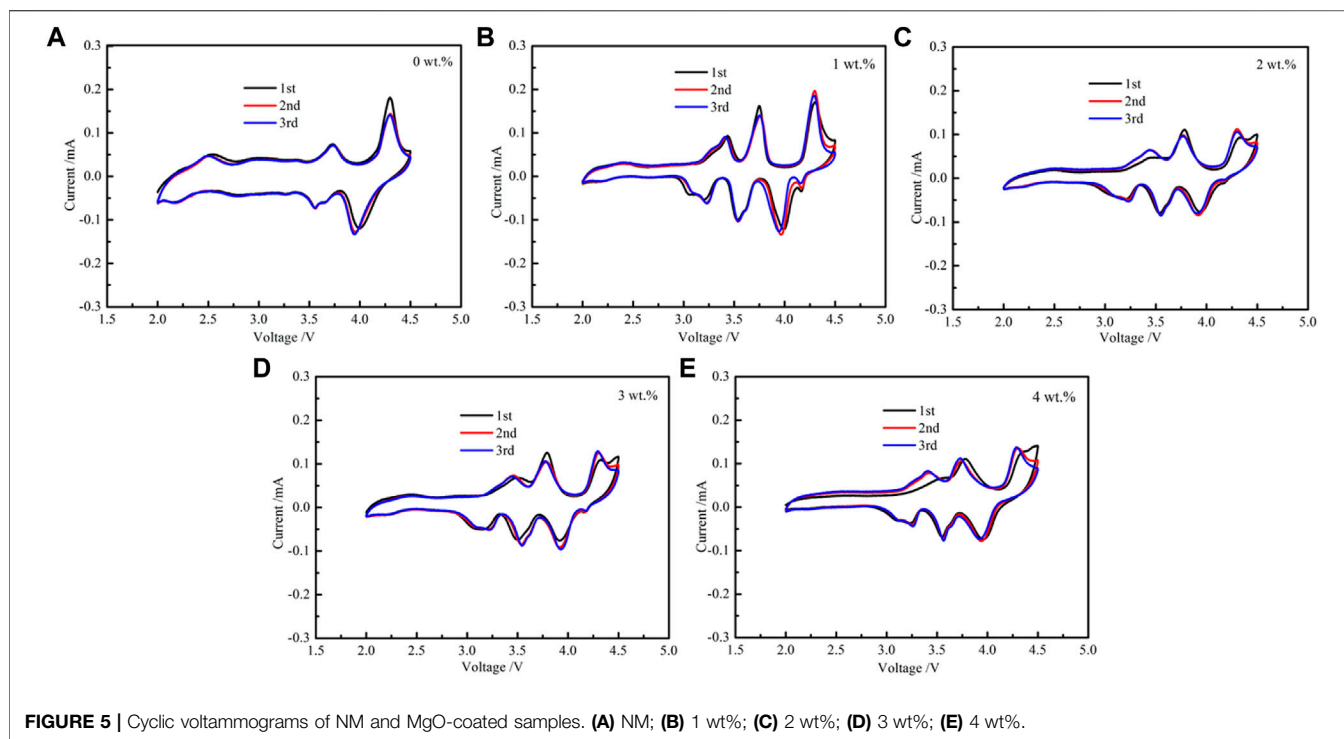
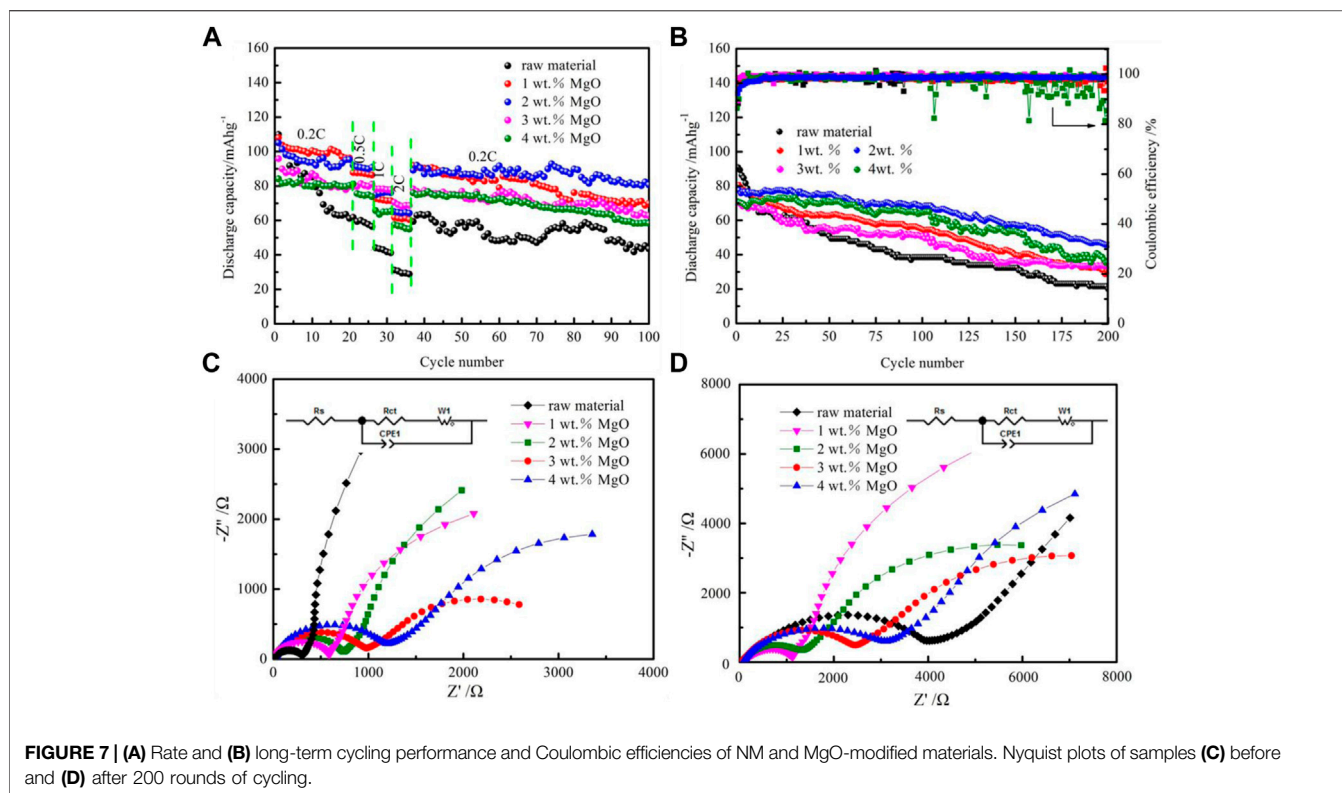


Figure 5 shows the CV plots of various electrodes at scanning rates of  $0.1 \text{ mV s}^{-1}$  ranging from 2 to 4.5 V. The reversible redox peaks at 3.4/3.25 V and 3.75/3.5 V are corresponding to the redox reaction of  $\text{Ni}^{2+}/\text{Ni}^{3+}$  and  $\text{Ni}^{3+}/\text{Ni}^{4+}$  (Yu et al., 2017).  $\text{Mn}^{3+}/\text{Mn}^{4+}$  peak couple are observed at low potentials ( $\leq 2.4 \text{ V}$ ) (Yuan et al.,

2013; Chen et al., 2018). The anodic/cathodic peaks at 4.25/4 V show more differences in intensity, indicating an irreversible electrochemical process, which can be related to the phase transition from P2 to O2 (Su et al., 2013; Liu et al., 2015). The CV curve of 2 wt%-coated samples own the highest coincidence



**FIGURE 7 | (A)** Rate and **(B)** long-term cycling performance and Coulombic efficiencies of NM and MgO-modified materials. Nyquist plots of samples **(C)** before and **(D)** after 200 rounds of cycling.

**TABLE 1 |** Comparison of initial capacity and cycling stability of layer cathodes modified by coating in recent reports.

Electrodes	Coating layer	Initial capacity (mAh g <sup>-1</sup> )	Capacity retention (mAh g <sup>-1</sup> )	References
Na <sub>2/3</sub> Ni <sub>1/3</sub> Mn <sub>2/3</sub> O <sub>2</sub>	MgO	105	81.5% (0.2 C 100 cycles)	This work
Na <sub>2/3</sub> Ni <sub>1/3</sub> Mn <sub>2/3</sub> O <sub>2</sub>	CuO	107	70.5% (0.1 C 100 cycles)	Dang et al. (2019)
Na <sub>0.66</sub> (Mn <sub>0.54</sub> Co <sub>0.13</sub> Ni <sub>0.13</sub> )O <sub>2</sub>	ZrO <sub>2</sub>	122	<50% (1 C 100 cycles)	Kaliyappan et al. (2017)
	TiO <sub>2</sub>	106	<50% (1 C 100 cycles)	
Na <sub>2/3</sub> Ni <sub>1/3</sub> Mn <sub>2/3</sub> O <sub>2</sub>	ZnO	94	75.4% (0.5 C 200 cycles)	Yang et al. (2020)
NaMn <sub>0.33</sub> Fe <sub>0.33</sub> Ni <sub>0.33</sub> O <sub>2</sub>	TiO <sub>2</sub>	103.6	71.0% (1 C 100 cycles)	Yu et al. (2020)

degree in the first 3 weeks. Compared with other samples, it shows better cyclic stability of the electrode under high voltage.

The charge and discharge tests of NM and MgO-coated samples are conducted at 0.2 C as presented in **Figure 6**. It is worth noting that the initial discharge capacities of pristine and MgO-NM (the MgO is 1, 2, 3, and 4 wt%) are 110, 108, 105, 96, and 84 mAh g<sup>-1</sup>, respectively. Furthermore, the capacity retention rates after 100 cycles are 78.2%, 81.5%, 87.6%, 76%, and 71.4%, respectively. However, the sample has the best capacity retention when the MgO coating thickness is 2 wt% compared with other samples.

The rate properties and cycling stability are important factors affecting the commercial application of SIBs. The rate performance and cycling stability of materials are revealed in **Figure 7**. As a result, the capability rate of all samples is analyzed within a 2.0–4.5-V voltage range at current densities from 0.2 to 2 C. As shown in **Figure 7A**, 2 wt% MgO-coated materials have the best performance rate among various materials. When the current density reaches up to 2 C, the average discharge capacity

of the material is about 66 mAh g<sup>-1</sup>. However, after a large current density cycle, the material still remains at 89 mAh g<sup>-1</sup> reversible specific capacity at 0.2 C in the 100th cycle, which is significantly higher than any other coated thickness samples. **Figure 7B** displays the cycling performance of the above samples at 0.5 C. The capacity of the pristine sample NM decreases the most. However, the 2 wt% MgO-coated sample exhibits an 84-mAh g<sup>-1</sup> initial discharge capacity at 0.5 C with a capacity retention of 66.7% after 200 cycles. Based on the foregoing, when the MgO coating thickness is 2 wt%, the comprehensive electrochemical performance of the material is the best. All results show that MgO with an appropriate thickness improves the conductivity and cycling stability of the pristine. **Table 1** is listed to intuitively show the comparison of the initial capacity and cycling stability of layer cathodes modified by coating in recent reports.

The performances of conductivity and charge transport of the above electrodes are investigated using electrochemical impedance spectroscopy measurements from 100 kHz to

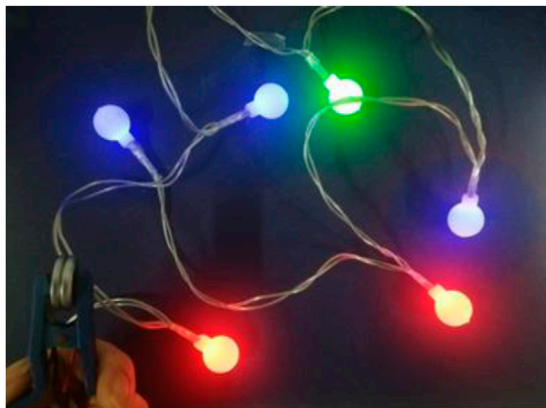


**FIGURE 8** | Digital photograph of colored LEDs lighted by two 2 wt% MgO-coated NM devices.

0.01 Hz as presented in **Figures 7C,D**. Nyquist plots are composed of one semicircle and a sloped straight line. In the middle and high frequencies, the diameter of the impedance curve represents the charge transfer impedance ( $R_{ct}$ ). The lowest  $R_{ct}$  values of samples indicate that they have the highest conductivity and fastest charge transfer rate. It should be noted that the  $R_{ct}$  value of the pristine sample increases sharply. However, the growth trend of  $R_{ct}$  has been significantly inhibited due to the existence of an MgO coating layer. The results suggest that a thin MgO coating layer can effectively alleviate electrode dissolution and prevent the formation of SEI film on the surface of the active material, so as to enhancing the long-term cycling performance of the material. Hence, considering the charge and discharge, rate, and long-term cycling performances, comprehensively, the cathodic material with 2 wt% MgO/NM has the best electrochemical performance. The 2 wt% MgO-coated NM was used as a cathode material to assemble a battery pack with two SIB half-batteries in series as illustrated in **Figure 8**. As can be seen, the battery pack can light up six small LED bulbs. The result confirms that the as-prepared MgO-coated cathode materials have excellent electrochemical properties and practical application ability.

## REFERENCES

- Bao, S., Huang, Y.-y., Wang, J.-z., Luo, S.-h., Su, G.-q., and Lu, J.-l. (2021). High-operating Voltage, Long-Life Layered Oxides for Sodium Ion Batteries Enabled by Cosubstitution of Titanium and Magnesium. *ACS Sust. Chem. Eng.* 9, 2534–2542. doi:10.1021/acssuschemeng.0c08174
- Chang-Heum Jo, C.-H., Jo, J.-H., Yashiro, H., Kim, S.-J., Sun, Y.-K., and Myung, S.-T. (2018). Bioinspired Surface Layer for the Cathode Material of High-Energy-Density Sodium-Ion Batteries. *Adv. Energ. Mater.* 8, 1702942. doi:10.1002/aenm.201702942
- Chen, T., Liu, W., Gao, H., Zhuo, Y., Hu, H., Chen, A., et al. (2018). A P2-type  $\text{Na}_0.44\text{Mn}_0.6\text{Ni}_0.3\text{Cu}_0.1\text{O}_2$  Cathode Material with High Energy Density for Sodium-Ion Batteries. *J. Mater. Chem. A.* 6, 12582–12588. doi:10.1039/c8ta04791j

## CONCLUSION

In this paper, the layered cathode oxide material of NM was synthesized by a simple solid-state method. Different-thickness MgO/NM were further synthesized by using a facile wet chemistry route as the electrode material of SIBs. Owing to the presence of an MgO coating layer on the surface of NM cathode materials, which prevents direct contact with electrolyte, stabilizes the surface structure, and effectively improves the electrochemical performance of the pristine material, the results of electrochemical test show that the cycling stability and rate capability are greatly improved. The 2 wt% MgO-coated cathode has a smaller  $R_{ct}$  value, superior rate properties, and high cycling stability. Therefore, MgO modification is an effective strategy for layered cathode oxide and a promising candidate for practical applications in next-generation sodium batteries.

## DATA AVAILABILITY STATEMENT

The original contributions presented in the study are included in the article/Supplementary Material; further inquiries can be directed to the corresponding authors.

## AUTHOR CONTRIBUTIONS

LX: investigation and writing—original draft. SB: conceptualization and formal analysis. LY: data curation. YZ: formal analysis. JL: methodology, supervision, and writing—review and editing. YY: supervision. All authors contributed to the article and approved the submitted version.

## FUNDING

This work was supported by the National Natural Science Foundation, China (52071091, 52004121, and 52001081); the Open Program of State Key Laboratory of Metal Material for Marine Equipment and Application (SKLMEA-K202007); and the Outstanding Young Talents Program of University of Science and Technology Liaoning (2021YQ01).

- Dang, R., Li, Q., Chen, M., Hu, Z., and Xiao, X. (2019). CuO-Coated and  $\text{Cu}^{2+}$ -Doped Co-modified P2-type  $\text{Na}_2/3[\text{Ni}_1/3\text{Mn}_2/3]\text{O}_2$  for Sodium-Ion Batteries. *Phys. Chem. Chem. Phys.* 21, 314–321. doi:10.1039/c8cp06248j
- Devendrasinh, D., Reddy, M. V., and Indranil, B. (2021). Understanding the Effect of Zn Doping on Stability of Cobalt-free P2- $\text{Na}_{0.60}\text{Fe}_{0.5}\text{Mn}_{0.5}\text{O}_2$  Cathode for Sodium Ion Batteries. *Electrochem* 2, 323–334. doi:10.3390/electrochem2020023
- Du, G., and Pang, H. (2021). Recent Advancements in Prussian Blue Analogues: Preparation and Application in Batteries. *Energ. Storage Mater.* 36, 387–408. doi:10.1016/j.ensm.2021.01.006
- Essehli, R., Alkhateeb, A., Mahmoud, A., Boschini, F., Ben Yahia, H., Amin, R., et al. (2020). Optimization of the Compositions of Polyanionic Sodium-Ion Battery Cathode  $\text{NaFe}_2-x\text{V}_x(\text{PO}_4)(\text{SO}_4)_2$ . *J. Power Sourc.* 469, 228417. doi:10.1016/j.jpowsour.2020.228417

- González, A., Goikolea, E., Barrena, J. A., and Mysyk, R. (2016). Review on Supercapacitors: Technologies and Materials. *Renew. Sust. Energ. Rev.* 58, 1189–1206. doi:10.1016/j.rser.2015.12.249
- Hakim, C., Sabi, N., and Saadoun, I. (2021). Mixed Structures as a New Strategy to Develop Outstanding Oxides-Based Cathode Materials for Sodium Ion Batteries: A Review. *J. Energ. Chem.* 61, 47–60. doi:10.1016/j.jechem.2021.02.027
- Huang, Y., Fang, C., Zeng, R., Liu, Y., Zhang, W., Wang, Y., et al. (2017). In Situ-Formed Hierarchical Metal-Organic Flexible Cathode for High-Energy Sodium-Ion Batteries. *Chemsuschem* 10, 4704–4708. doi:10.1002/cssc.201701484
- Jae Hyeon Jo, J. H., Choi, J. U., Konarov, A., Yashiro, H., Yuan, S., Shi, L., et al. (2018). Sodium-Ion Batteries: Building Effective Layered Cathode Materials with Long-Term Cycling by Modifying the Surface via Sodium Phosphate. *Adv. Funct. Mater.* 28, 1705968. doi:10.1002/adfm.201705968
- Jin, T., Wang, P. F., Wang, Q. C., Zhu, K., Deng, T., Zhang, J., et al. (2020). Realizing Complete Solid-Solution Reaction in High Sodium Content P2-type Cathode for High-Performance Sodium-Ion Batteries. *Angew. Chem. Int. Ed.* 59, 14511–14516. doi:10.1002/anie.202003972
- Kaliyappan, K., Liu, J., Lushington, A., Li, R., and Sun, X. (2015). Highly Stable Na<sub>2</sub>/3(Mn<sub>0.54</sub>Ni<sub>0.13</sub>Co<sub>0.13</sub>)O<sub>2</sub> Cathode Modified by Atomic Layer Deposition for Sodium-Ion Batteries. *ChemSusChem* 8, 2537–2543. doi:10.1002/cssc.201500155
- Kaliyappan, K., Liu, J., Xiao, B., Lushington, A., Li, R., Sham, T.-K., et al. (2017). Enhanced Performance of P2-Na<sub>0.66</sub>(Mn<sub>0.54</sub>Co<sub>0.13</sub>Ni<sub>0.13</sub>)O<sub>2</sub> Cathode for Sodium-Ion Batteries by Ultrathin Metal Oxide Coatings via Atomic Layer Deposition. *Adv. Funct. Mater.* 27, 1701870–1701877. doi:10.1002/adfm.201701870
- Kannan, K., Kouthaman, M., Arjunan, P., Priyanka, V., Subadevi, R., Kumaresan, L., et al. (2021). Iron Substituted Layered P2-type Na<sub>1/2</sub>Ti<sub>6</sub>/10Ni<sub>3</sub>/10Fe<sub>1</sub>/10O<sub>2</sub> as Innovative Anode Material for Rechargeable Sodium Batteries. *Inorg. Chem. Commun.* 124, 108383. doi:10.1016/j.inoche.2020.108383
- Kuan Wang, K., Yan, P., and Sui, M. (2018). Phase Transition Induced Cracking Plaguing Layered Cathode for Sodium-Ion Battery. *Nano Energy* 54, 148–155. doi:10.1016/j.nanoen.2018.09.073
- Kundu, D., Talaie, E., Duffort, V., and Nazar, L. F. (2015). The Emerging Chemistry of Sodium Ion Batteries for Electrochemical Energy Storage. *Angew. Chem. Int. Ed.* 54, 3431–3448. doi:10.1002/chin.2015213091
- Lee, D. H., Xu, J., and Meng, Y. S. (2013). An Advanced Cathode for Na-Ion Batteries with High Rate and Excellent Structural Stability. *Phys. Chem. Chem. Phys.* 15, 3304–3312. doi:10.1039/c2cp44467d
- Li, J., Xiong, S., Liu, Y., Ju, Z., and Qian, Y. (2013). Uniform LiNi<sub>1/3</sub>Co<sub>1/3</sub>Mn<sub>1/3</sub>O<sub>2</sub> Hollow Microspheres: Designed Synthesis, Topotactical Structural Transformation and Their Enhanced Electrochemical Performance. *Nano Energy* 2, 1249–1260. doi:10.1016/j.nanoen.2013.06.003
- Lin, C., Zhang, Y., Chen, L., Lei, Y., Ou, J., Guo, Y., et al. (2015). Hydrogen Peroxide Assisted Synthesis of LiNi<sub>1/3</sub>Co<sub>1/3</sub>Mn<sub>1/3</sub>O<sub>2</sub> as High-Performance Cathode for Lithium-Ion Batteries. *J. Power Sourc.* 280, 263–271. doi:10.1016/j.jpowsour.2015.01.084
- Liu, G., Wen, L., Li, Y., and Kou, Y. (2015). Synthesis and Electrochemical Properties of P2-Na<sub>2</sub>/3Ni<sub>1</sub>/3Mn<sub>2</sub>/3O<sub>2</sub>. *Ionics* 21, 1011–1016. doi:10.1007/s11581-014-1249-2
- Lu, L., Han, X., Li, J., Hua, J., and Ouyang, M. (2013). A Review on the Key Issues for Lithium-Ion Battery Management in Electric Vehicles. *J. Power Sourc.* 226, 272–288. doi:10.1016/j.jpowsour.2012.10.060
- Lv, Z., Ling, M., Yue, M., Li, X., Song, M., Zheng, Q., et al. (2021). Vanadium-based Polyanionic Compounds as Cathode Materials for Sodium-Ion Batteries: Toward High-Energy and High-Power Applications. *J. Energ. Chem.* 55, 361–390. doi:10.1016/j.jechem.2020.07.008
- Peng, L., Zhu, Y., Chen, D., Ruoff, R. S., and Yu, G. (2016). Two-Dimensional Materials for Beyond-Lithium-Ion Batteries. *Adv. Energ. Mater.* 6, 1600025. doi:10.1002/aenm.201600025
- Peng-Fei Wang, P.-F., Yao, H.-R., Liu, X.-Y., Yin, Y.-X., Zhang, J.-N., Wen, Y., et al. (2018). Na +/vacancy Disorder Promises High-Rate Na-Ion Batteries. *Sci. Adv.* 4, eaar6018. doi:10.1126/sciadv.aar6018
- Pu, X., Wang, H., Zhao, D., Yang, H., Ai, X., Cao, S., et al. (2019). Recent Progress in Rechargeable Sodium-Ion Batteries: toward High-Power Applications. *Small* 15, 1805427. doi:10.1002/sml.201805427
- Rong, X., Qi, X., Lu, Y., Wang, Y., Li, Y., Jiang, L., et al. (2019). A New Tin-Based O<sub>3</sub>-Na<sub>0.9</sub>[Ni<sub>0.45</sub>-2Mn Sn<sub>0.55</sub>-2]O<sub>2</sub> as Sodium-Ion Battery Cathode. *J. Energ. Chem.* 31, 132–137. doi:10.1016/j.jechem.2018.05.019
- Shi, S. J., Tu, J. P., Tang, Y. Y., Liu, X. Y., Zhang, Y. Q., Wang, X. L., et al. (2013). Enhanced Cycling Stability of Li[Li<sub>0.2</sub>Mn<sub>0.54</sub>Ni<sub>0.13</sub>Co<sub>0.13</sub>]O<sub>2</sub> by Surface Modification of MgO with Melting Impregnation Method. *Electrochimica Acta* 88, 671–679. doi:10.1016/j.electacta.2012.10.111
- Su, D., Wang, C., Ahn, H.-j., and Wang, G. (2013). Single Crystalline Na<sub>0.7</sub>MnO<sub>2</sub> Nanoplates as Cathode Materials for Sodium-Ion Batteries with Enhanced Performance. *Chem. Eur. J.* 19, 10884–10889. doi:10.1002/chem.201301563
- Tanabe, D., Shimono, T., Kobayashi, W., and Moritomo, Y. (2013). Na-site Energy of P2-type Na<sub>x</sub>MO<sub>2</sub>(M= Mn and Co). *Phys. Status Solidi RRL* 7, 1097–1101. doi:10.1002/pssr.201308101
- Wang, S., Wang, L., Zhu, Z., Hu, Z., Zhao, Q., and Chen, J. (2014). All Organic Sodium-Ion Batteries with Na<sub>4</sub>C<sub>8</sub>H<sub>2</sub>O<sub>6</sub>. *Angew. Chem. Int. Ed.* 53, 5892–5896. doi:10.1002/anie.201400032
- Wang, P.-F., You, Y., Yin, Y.-X., Wang, Y.-S., Wan, L.-J., Gu, L., et al. (2016). Suppressing the P2-O2 Phase Transition of Na<sub>0.67</sub>Mn<sub>0.67</sub>Ni<sub>0.33</sub>O<sub>2</sub> by Magnesium Substitution for Improved Sodium-Ion Batteries. *Angew. Chem. Int. Ed.* 55, 7445–7449. doi:10.1002/anie.201602202
- Wu, X., Guo, J., Wang, D., Zhong, G., McDonald, M. J., Yang, Y., et al. (2015). P2-type Na<sub>0.66</sub>Ni<sub>0.33-x</sub>Zn<sub>x</sub>Mn<sub>0.67</sub>O<sub>2</sub> as New High-Voltage Cathode Materials for Sodium-Ion Batteries. *J. Power Sourc.* 281, 18–26. doi:10.1016/j.jpowsour.2014.12.083
- Yang, Y., Dang, R., Wu, K., Li, Q., Li, N., Xiao, X., et al. (2020). Semiconductor Material ZnO-Coated P2-type Na<sub>2</sub>/3Ni<sub>1</sub>/3Mn<sub>2</sub>/3O<sub>2</sub> Cathode Materials for Sodium-Ion Batteries with Superior Electrochemical Performance. *J. Phys. Chem. C* 124, 1780–1787. doi:10.1021/acs.jpcc.9b08220
- Yang, Y., and Wei, W.-F. (2020). Electrochemical Mechanism of High Na-Content P2-type Layered Oxides for Sodium-Ion Batteries. *Rare Met.* 39, 332–334. doi:10.1007/s12598-020-01403-7
- Yu, T.-Y., Hwang, J.-Y., Aurbach, D., and Sun, Y.-K. (2017). Microsphere Na<sub>0.65</sub>[Ni<sub>0.17</sub>Co<sub>0.11</sub>Mn<sub>0.72</sub>]O<sub>2</sub> Cathode Material for High-Performance Sodium-Ion Batteries. *ACS Appl. Mater. Inter.* 9, 44534–44541. doi:10.1021/acsmi.7b15267
- Yu, Y., Kong, W., Li, Q., Ning, D., Schuck, G., Schumacher, G., et al. (2020). Understanding the Multiple Effects of TiO<sub>2</sub> Coating on NaMn<sub>0.33</sub>Fe<sub>0.33</sub>Ni<sub>0.33</sub>O<sub>2</sub> Cathode Material for Na-Ion Batteries. *ACS Appl. Energ. Mater.* 3, 933–942. doi:10.1021/acsaem.9b02021
- Yuan, D., He, W., Pei, F., Wu, F., Wu, Y., Qian, J., et al. (2013). Synthesis and Electrochemical Behaviors of Layered Na<sub>0.67</sub>[Mn<sub>0.65</sub>Co<sub>0.2</sub>Ni<sub>0.15</sub>]O<sub>2</sub> Microflakes as a Stable Cathode Material for Sodium-Ion Batteries. *J. Mater. Chem. A* 1, 3895–3899. doi:10.1039/c3ta01430d
- Zhao, C., Wang, Q., Yao, Z., Wang, J., Sánchez-Lengeling, B., Ding, F., et al. (2020). Rational Design of Layered Oxide Materials for Sodium-Ion Batteries. *Science* 370, 708–711. doi:10.1126/science.aay9972
- Zhao, X., Fan, L.-Z., and Zhou, Z. (2021). Cationic Potential: An Effective Descriptor for Rational Design of Layered Oxides for Sodium-Ion Batteries. *Green. Energ. Environ.* 6, 455–457. doi:10.1016/j.gjee.2020.11.022
- Zhu, Y., Wang, B., Gan, Q., Wang, Y., Wang, Z., Xie, J., et al. (2019). Selective Edge Etching to Improve the Rate Capability of Prussian Blue Analogues for Sodium Ion Batteries. *Inorg. Chem. Front.* 6, 1361–1366. doi:10.1039/c9qj00090a

**Conflict of Interest:** The authors declare that the research was conducted in the absence of any commercial or financial relationships that could be construed as a potential conflict of interest.

**Publisher's Note:** All claims expressed in this article are solely those of the authors and do not necessarily represent those of their affiliated organizations, or those of the publisher, the editors, and the reviewers. Any product that may be evaluated in this article, or claim that may be made by its manufacturer, is not guaranteed or endorsed by the publisher.

Copyright © 2022 Xue, Bao, Yan, Zhang, Lu and Yin. This is an open-access article distributed under the terms of the Creative Commons Attribution License (CC BY). The use, distribution or reproduction in other forums is permitted, provided the original author(s) and the copyright owner(s) are credited and that the original publication in this journal is cited, in accordance with accepted academic practice. No use, distribution or reproduction is permitted which does not comply with these terms.